HEFAT2008
6th International Conference on Heat Transfer, Fluid Mechanics and Thermodynamics
30 June to 2 July 2008
Pretoria, South Africa
Paper number: CM4

LAMINAR NATURAL CONVECTION HEAT TRANSFER FROM VERTICAL AND INCLINED PLATES FACING UPWARDS AND DOWNWARDS

C. Cianfrini[a], M. Corcione [a,]*, A. D'Orazio[b] and E. Habib[a]
*Author for correspondence
[a]Dipartimento di Fisica Tecnica, "Sapienza" University of Rome
via Eudossiana, 18 – 00184 Rome, Italy
[b]Dipartimento di Meccanica e Aeronautica, "Sapienza" University of Rome
via Eudossiana, 18 – 00184 Rome, Italy
e-mail: massimo.corcione@uniroma1.it

ABSTRACT

Steady laminar natural convection heat transfer from thin isothermal plates inclined with respect to the gravity vector, for both cases of heated side facing either upwards or downwards, is studied numerically. A computer code based on the SIMPLE-C algorithm is used for the solution of the mass, momentum, and energy conservation equations. Simulations are performed for different values of the inclination angle of the plate in the range between −75deg and +75deg, the Rayleigh number in the range between 10^1 and 10^8, and the Prandtl number in the range between 0.7 and 70, whose effects on the temperature and flow fields, and on the heat transfer rate, are analyzed in detail and discussed.

INTRODUCTION

Free convection heat transfer from flat plates has been the subject of numerous theoretical and experimental studies, being of interest in a variety of industrial applications. In addition to the limiting cases of flow adjacent to vertical and horizontal surfaces, the intermediate case of inclined plates has also been examined by a number of investigators, mainly experimentally, for both cases of uniform wall temperature and uniform heat flux at the plate surface, see, e.g., references [1] to [11].

However, a non-negligible discrepancy among the several heat transfer results available in the literature may be detected. In particular, such discrepancy, which increases with the plate inclination, may also amount to ±50%, or more, depending on the investigation method, the boundary conditions, and the occurrence of more or less pronounced three-dimensional edge-effects. Thus, information is sometimes inconsistent.

Moreover, the fluids traditionally used in experiments were only air and water, which implies a shortness of data for liquids with Pr > 10, e.g., dielectric coolants and silicone oils. On the other hand, the results of the theoretical studies based on the boundary-layer approach, which are virtually applicable to any type of fluid, become inapplicable at low Rayleigh numbers.

It is therefore felt the need of a systematic investigation on natural convection heat transfer from tilted plates facing either upwards or downwards, and suspended in different types of fluids, which is the scope of the present paper.

The study is carried out numerically under the assumption of steady, two-dimensional laminar flow. The case of uniform wall temperature is considered. A computer code based on the SIMPLE-C algorithm is employed for the solution of the mass, momentum and energy conservation equations. Simulations are performed for different values of the Rayleigh number in the range between 10^1 and 10^8, the angle of inclination to gravity in the range between −75deg and +75deg, and the Prandtl number in the range between 0.7 and 70, whose effects on the flow and temperature fields, and on the heat transfer rate, are analyzed in detail and discussed. Dimensionless heat transfer correlations are also developed.

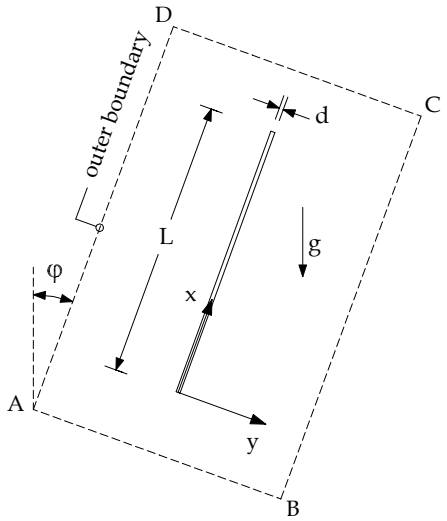

Figure 1 – Geometry, coordinate system and integration domain

PROBLEM FORMULATION

A plate of length L, inclined of an angle φ with respect to gravity, is considered. The plate thickness d is set at 1/50 of its length. One side of the plate is kept at uniform temperature t_p, whereas the opposite side and both ends are perfectly insulated. Free convection heat transfer occurs between the heated surface of the plate and the surrounding undisturbed fluid, assumed at uniform temperature t_∞.

The flow is assumed steady, two-dimensional, laminar, and incompressible, with constant fluid properties and negligible viscous dissipation and pressure work. The buoyancy effects on momentum transfer are taken into account by the Boussinesq approximation.

Governing equations

Once the above assumptions are used in the conservation equations of mass, momentum and energy, the following set of dimensionless governing equations is obtained:

$$\nabla \cdot \mathbf{V} = 0 \tag{1}$$

$$(\mathbf{V}\cdot\nabla)\mathbf{V} = -\nabla p + \nabla^2 \mathbf{V} - \frac{\mathrm{Ra}}{\mathrm{Pr}} \mathrm{T} \frac{\mathbf{g}}{g} \tag{2}$$

$$(\mathbf{V}\cdot\nabla)\mathrm{T} = \frac{1}{\mathrm{Pr}}\nabla^2 \mathrm{T} \tag{3}$$

where **V** is the dimensionless velocity vector with components U and V, parallel and perpendicular to the plate, respectively, normalized with ν/L; T is the dimensionless temperature excess over the temperature of the undisturbed fluid normalized with the temperature difference $(t_p - t_\infty)$; p is the dimensionless pressure normalized with $\rho_\infty \nu^2/L^2$; Ra is the Rayleigh number based on the length of the plate; and Pr is the Prandtl number.

The related boundary condition are T = 1 and **V** = 0 at the heated side of the plate, $\partial T/\partial n = 0$ and **V** = 0 at the insulated side and both ends of the plate (n detotes the direction normal to the surface), and T = 0 and **V** = 0 at very large distance from the plate.

Computational domain and boundary conditions

The finite-difference solution of equations (1)–(3) with the boundary conditions stated above requires that a computational domain is established. The two-dimensional integration domain is taken as a rectangle which includes the plate and extends sufficiently far from it, as sketched in Fig. 1, where the (x,y) Cartesian coordinate system adopted is also represented. Such integration domain is filled with a non-uniform grid, having a concentration of grid lines near the plate. As regards the boundary conditions to be assigned at the four lines which enclose the rectangular integration domain, once these lines are set sufficiently far from the plate, the motion of the fluid which enters or leaves the computational domain may reasonably be assumed to occur normally to them. The entering fluid is assumed at the undisturbed free field temperature. In contrast, for the leaving fluid, whose temperature is not known a priori, a zero temperature gradient along the normal to the boundary line is assumed. Accordingly, the following boundary conditions are applied (see Fig. 1):

a) at the heated side of the plate

$$\mathrm{U} = 0\,, \quad \mathrm{V} = 0\,, \quad \mathrm{T} = 1 \tag{4}$$

b) at the insulated side of the plate

$$\mathrm{U} = 0\,, \quad \mathrm{V} = 0\,, \quad \frac{\partial \mathrm{T}}{\partial \mathrm{Y}} = 0 \tag{5}$$

c) at both ends of the plate

$$\mathrm{U} = 0\,, \quad \mathrm{V} = 0\,, \quad \frac{\partial \mathrm{T}}{\partial \mathrm{X}} = 0 \tag{6}$$

d) at boundary line A–B

$$\frac{\partial \mathrm{U}}{\partial \mathrm{X}} = 0\,, \quad \mathrm{V} = 0\,, \quad \mathrm{T} = 0 \ \text{if} \ \mathrm{U} \geq 0 \ \text{or} \ \frac{\partial \mathrm{T}}{\partial \mathrm{X}} = 0 \ \text{if} \ \mathrm{U} < 0 \tag{7}$$

e) at boundary line B–C

$$\mathrm{U} = 0\,, \quad \frac{\partial \mathrm{V}}{\partial \mathrm{Y}} = 0\,, \ \mathrm{T} = 0 \ \text{if} \ \mathrm{V} < 0 \ \text{or} \ \frac{\partial \mathrm{T}}{\partial \mathrm{Y}} = 0 \ \text{if} \ \mathrm{V} \geq 0 \tag{8}$$

f) at boundary line C–D

$$\frac{\partial \mathrm{U}}{\partial \mathrm{X}} = 0\,, \quad \mathrm{V} = 0\,, \quad \mathrm{T} = 0 \ \text{if} \ \mathrm{U} < 0 \ \text{or} \ \frac{\partial \mathrm{T}}{\partial \mathrm{X}} = 0 \ \text{if} \ \mathrm{U} \geq 0 \tag{9}$$

g) at boundary line A–D

$$\mathrm{U} = 0\,, \quad \frac{\partial \mathrm{V}}{\partial \mathrm{Y}} = 0\,, \ \mathrm{T} = 0 \ \text{if} \ \mathrm{V} \geq 0 \ \text{or} \ \frac{\partial \mathrm{T}}{\partial \mathrm{Y}} = 0 \ \text{if} \ \mathrm{V} < 0 \tag{10}$$

in which X and Y are the dimensionless Cartesian coordinates, normalized with L.

Solution algorithm

The set of equations (1)–(3) with the boundary conditions (4)–(10) is solved numerically by a control-volume formulation of the finite-difference method. The pressure-velocity coupling is handled through the SIMPLE-C algorithm by Van Doormaal and Raithby [12]. The advection fluxes are evaluated by the QUICK discretization scheme by Leonard [13]. Starting from first-approximation distributions of the dependent variables, the discretized governing equations are solved iteratively via a line-by-line application of the Thomas algorithm, enforcing under-relaxation to ensure convergence. The solution is considered to be converged when the maximum absolute values of the mass source and the percentage changes of the dependent variables at any grid-node between two consecutive iterations are smaller than the prescribed values, i.e., 10^{-4} and 10^{-6}, respectively.

Data reduction

After convergence is attained, the local and average Nusselt numbers Nu and Nu_{av} are calculated:

$$\mathrm{Nu} = \frac{\mathrm{qL}}{\mathrm{k}(t_p - t_\infty)} = -\left.\frac{\partial \mathrm{T}}{\partial \mathrm{Y}}\right|_{\mathrm{Y}=\mathrm{d}/2\mathrm{L}} \tag{11}$$

$$Nu_{av} = \frac{Q}{k(t_p - t_\infty)} = -\int_0^1 \left(\frac{\partial T}{\partial Y}\bigg|_{Y=d/2L}\right) dX \qquad (12)$$

where q is the heat flux and Q is the heat transfer rate. The temperature gradients at the heated surface of the plate are evaluated by a second-order profile among each wall-node and the next two fluid-nodes. The integrals are approximated by the trapezoid rule.

Validation of the numerical procedure

Tests on the dependence of the results on the mesh-spacing, as well as on the extent of the computational domain, have been performed for several combinations of values of Ra, φ, and Pr. This has brought to determine the grid-spacings and the extents of the integration domain used for computations, which are such that further refinements of the grid or enlargements of the computational domain do not yield for noticeable modifications neither in the heat transfer rate nor in the flow field, that is, the percentage changes of Nu and Nu_{av}, and the percentage changes of the maximum value of the velocity component U at X = L/4, L/2 and 3L/4, are smaller than the prescribed accuracy values, i.e., 1% and 2%, respectively. Typical features of the integration domain may be summarized as follows: (a) the number of nodal points lies in the range between 50×100 and 100×400, (b) the extent of the integration domain ranges between 2L and 8L upwards, between L and 3L downwards, and between L and 5L sidewards, depending on Ra, φ, and Pr.

As far as the validation of the numerical code is concerned, a comparison among the average Nusselt numbers obtained for a vertical plate at different Rayleigh and Prandtl numbers and the corresponding values derived from both the Churchill-Chu correlation based on experimental data by other authors [14] and the Raithby-Hollands theoretical equation [15], is reported in Table 1. In addition, the average Nusselt numbers obtained for a tilted plate in air at Ra = 1.7×10^6 are compared with the values derived from the Hassan-Mohamed correlation based on their experimental results [2], as shown in Tables 2 and 3 for positive and negative inclination angles, respectively.

Table 1 – Comparison of the present solutions for the average Nusselt number of a vertical plate and the data derived from the Churchill-Chu and Raithby-Hollands correlating equations

Ra	φ = 0°	Nu		
		Pr = 0.7	7	70
10^2	Present	2.52	2.79	2.88
	Churchill-Chu eqn [14]	2.30	2.62	2.74
	Raithby-Hollands eqn [15]	2.81	3.14	3.28
10^4	Present	5.88	6.68	7.05
	Churchill-Chu eqn [14]	5.81	6.80	7.20
	Raithby-Hollands eqn [15]	6.43	7.43	7.84
10^6	Present	17.47	19.67	20.76
	Churchill-Chu eqn [14]	16.92	20.04	21.30
	Raithby-Hollands eqn [15]	17.55	20.67	21.93

Table 2 – Comparison of the present solutions for the average Nusselt number of a positively inclined plate and the Hassan-Mohamed data

Ra = 1.7×10^6, Pr = 0.7	Nu_{av}			
	φ = +15°	+30°	+45°	+60°
Present	19.02	18.60	17.82	16.61
Hassan-Mohamed eqn [2]	18.14	17.65	16.78	15.39

Table 3 – Comparison of the present solutions for the average Nusselt number of a negatively inclined plate and the Hassan-Mohamed data

Ra = 1.7×10^6, Pr = 0.7	Nu_{av}			
	φ = –15°	–30°	–45°	–60°
Present	18.91	18.38	17.46	16.06
Hassan-Mohamed eqn [2]	18.14	17.65	16.78	15.39

It may be seen that the Churchill-Chu correlation at low and moderate Rayleigh numbers, as well as the Hassan-Mohamed correlation, underpredict slightly the present Nusselt numbers, while the Raithby-Hollands equation tends to overpredict them. However, this was expected, since, at the Rayleigh numbers considered, the Churchill-Chu and Hassan-Mohamed equations fall slightly below the experimental data upon which they were based, while the predictions of the Raithby-Hollands equation are somewhat higher than several literature experimental data.

In addition, also the velocity distributions – not reported for the sake of brevity – have shown a substantially good degree of agreement with the experimental data by Kierkus [1] for tilting angles in the range between –45deg and +45deg.

DISCUSSION OF THE RESULTS

Numerical simulations are performed for different values of the Rayleigh number, Ra, in the range between 10^1 and 10^8, the inclination angle of the plate, φ, in the range between –75deg and +75deg (the heated side of the plate faces downwards or upwards according as the tilting angle is negative or positive), and the Prandtl number, Pr, in the range between 0.7 and 70.

Heat transfer features

A selection of local results is presented in Fig. 2, where a set of isotherm contours are plotted for Ra = 10^4 and Pr = 0.7, in order to highlight in what measure the tilting angle of the plate affects the heat transfer performance (the respective flow field plots are omitted for briefness).

It is apparent how, for downward-facing plates, the effect of angle φ is to increase the thickness of the boundary layer at the leading edge of the plate; moreover, at large inclination angles, the boundary layer at the trailing edge of the plate becomes slightly thinner, being squeezed towards the plate surface by the buoyant action of the plume, that is evident at φ = –60deg and –75deg. In contrast, for upward-facing plates, the effect of the inclination angle φ is to thicken the tail end of the boundary layer, and to give the wall jet a tendency to separate from the surface, which is clearly evident at φ = +75deg. Of course, these effects have a direct influence on the local heat fluxes, as shown in Figs. 3 and 4, where the distributions of Nu along the plate for Ra = 10^4 and Pr = 0.7, are represented for plates facing downwards and upwards, respectively.

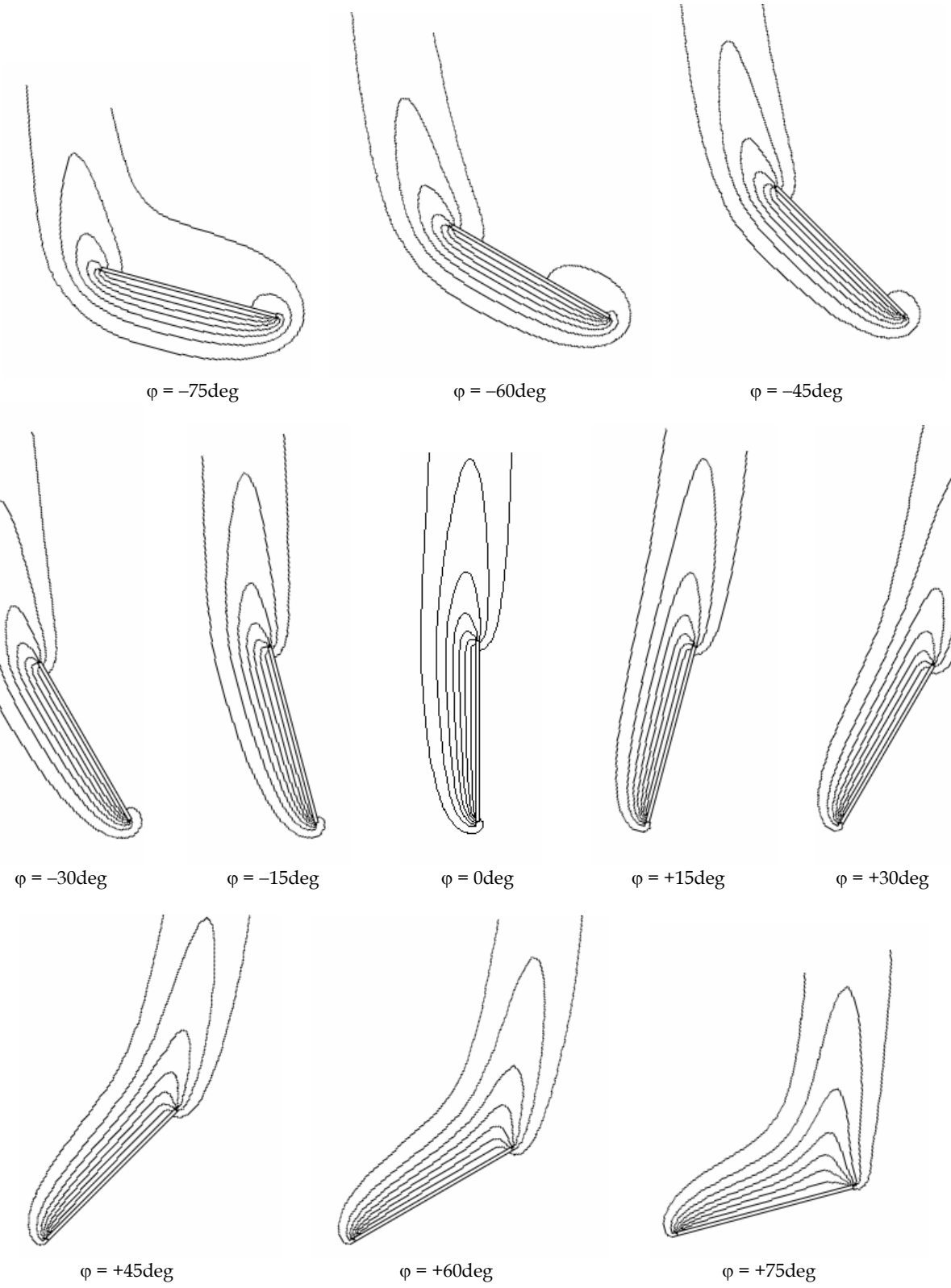

Figure 2 – Effects of the tilting angle: isotherm lines for Ra = 10^4, Pr = 0.7, and φ in the range from –75deg to +75deg

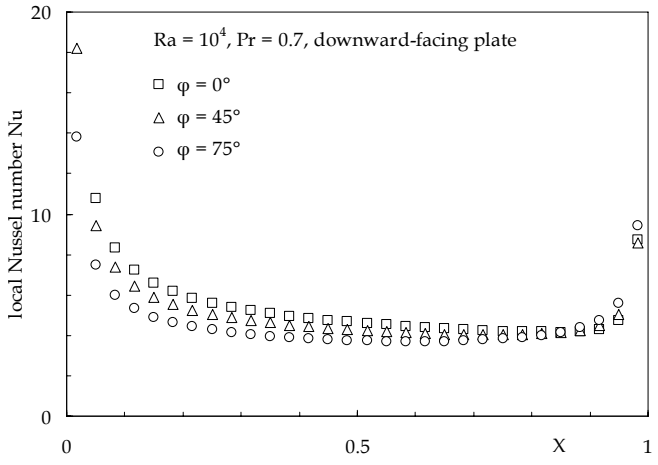

Figure 3 – Distributions of Nu along the plate for Ra = 10^4, Pr = 0.7 and different negative tilting angles φ (downward-facing plates)

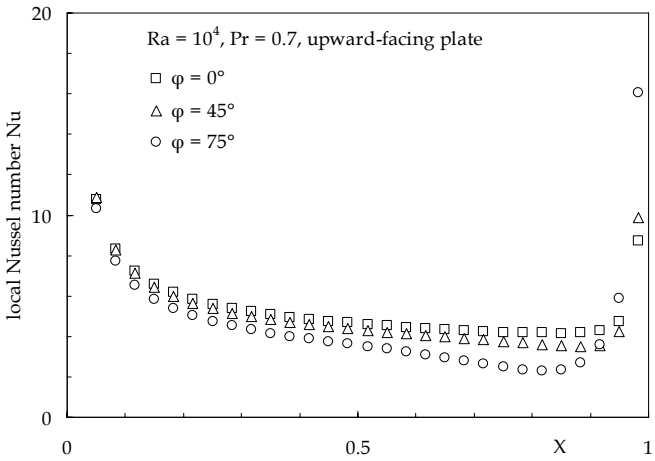

Figure 4 – Distributions of Nu along the plate for Ra = 10^4, Pr = 0.7 and different positive tilting angles φ (upward-facing plates)

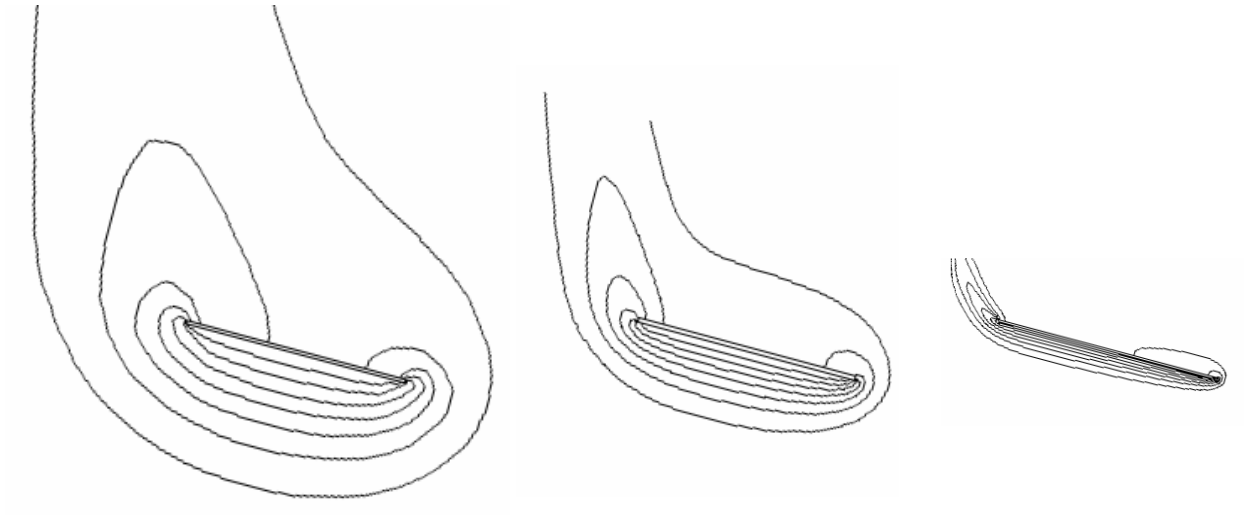

Figure 5 – Effects of the Rayleigh number: isotherm lines for φ = –75deg, Pr = 0.7, and Ra = 10^2, 10^4, and 10^6

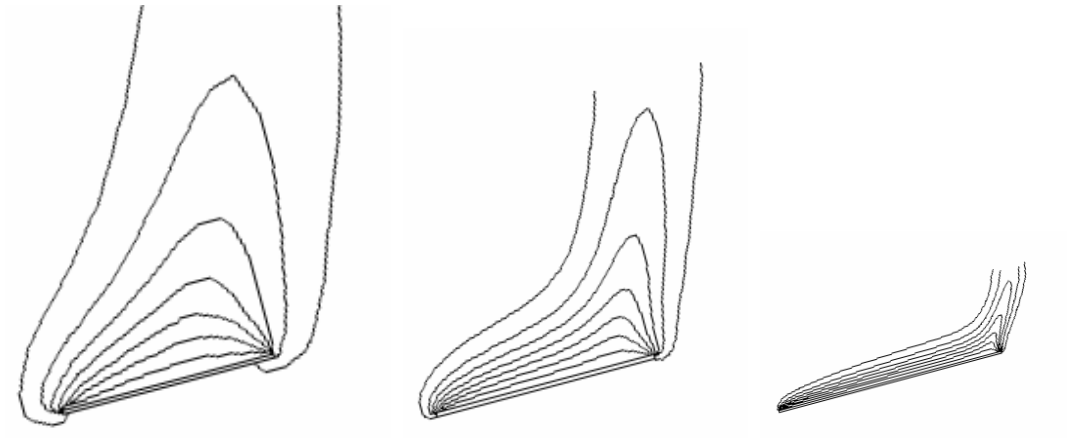

Figure 6 – Effects of the Rayleigh number: isotherm lines for φ = +75deg, Pr = 0.7, and Ra = 10^2, 10^4, and 10^6

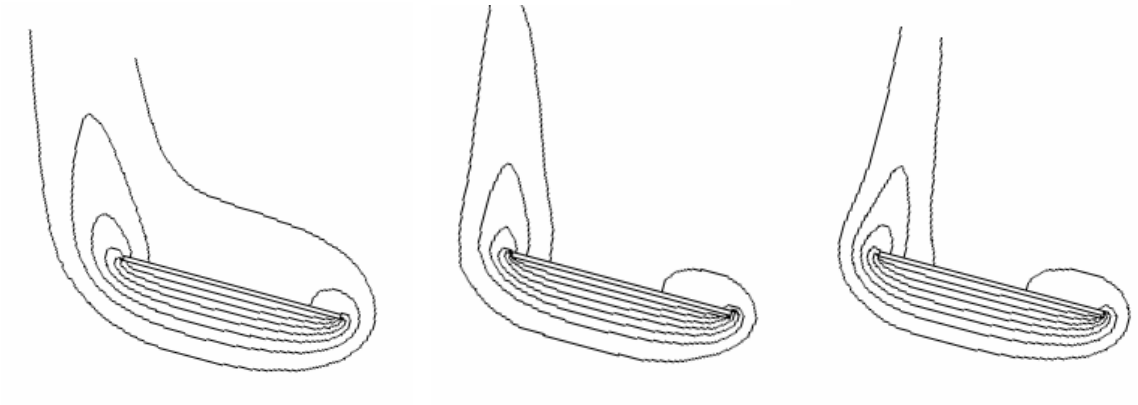

Figure 7 – Effects of the Prandtl number: isotherm lines for $\varphi = -75$deg, $Ra = 10^4$, and $Pr = 0.7$, 7, and 70

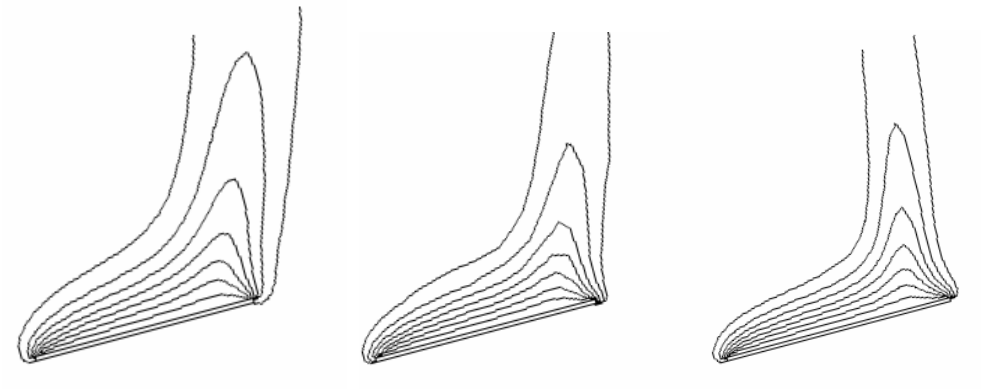

Figure 8 – Effects of the Prandtl number: isotherm lines for $\varphi = +75$deg, $Ra = 10^4$, and $Pr = 0.7$, 7, and 70

The effects of the Rayleigh and Prandtl numbers are pointed out in Figs. 5–6 and 7–8, respectively, where sets of equispaced isotherm contours are plotted for ±75deg inclination angles and different values of Ra and Pr. The typical decrease in thickness of the boundary layer occurring as both Ra and Pr increase may be noticed; in addition, the buoyant plume shrinks and rotates – outwards with increasing Ra, and inwards with increasing Pr –, the latter effect being more noticeable for the downward-facing configuration. Furthermore, at large positive tilting angles (then for plates facing upwards), the root of the plume shifts towards the trailing edge of the plate as the Rayleigh number increases.

Heat transfer correlations

A correlation for the local heat transfer performance of the plate, with a functional structure derived from the expression originally proposed for vertical plates by Churchill and Usagi [16], has been developed in terms of Nu_x and $Ra_x \cos\varphi$, where the local Nusselt number $Nu_x = qx / k(t_p - t_\infty)$ is obtained from the local Nusselt number Nu defined in eq. (11) by replacing the length L of the plate with the distance x from the leading edge, while Ra_x is the local Rayleigh number based on x:

$$Nu_x = \frac{0.48}{\left[1 + (0.618/Pr)^{9/16}\right]^{9/25}} (Ra_x \cos\varphi)^{0.25} \qquad (13)$$

for $-75\text{deg} \le \varphi \le 60\text{deg}$, $10^2 \le Ra \le 10^6$, $0.1 \le x / L \le 0.9$ and $0.7 \le Pr \le 70$, with a 5.7% standard deviation of error, and a ±10% range of error with a 90% level of confidence, as shown in Fig. 9 – where, for the sake of clarity, less than one-fourth of the data used for deriving eq. (13) is represented.

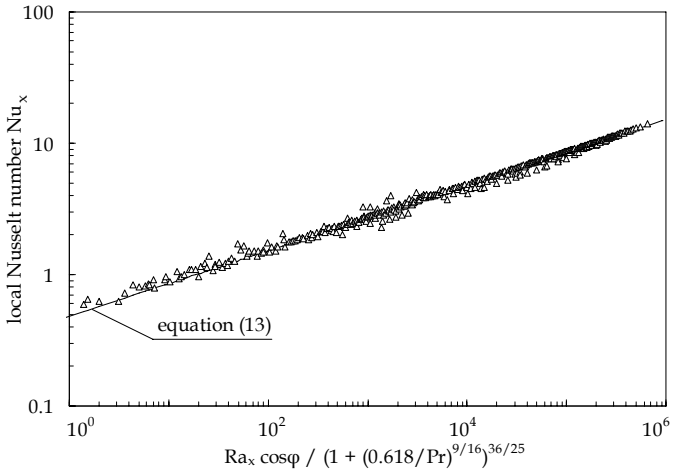

Figure 9 – Correlating equation for the local heat transfer

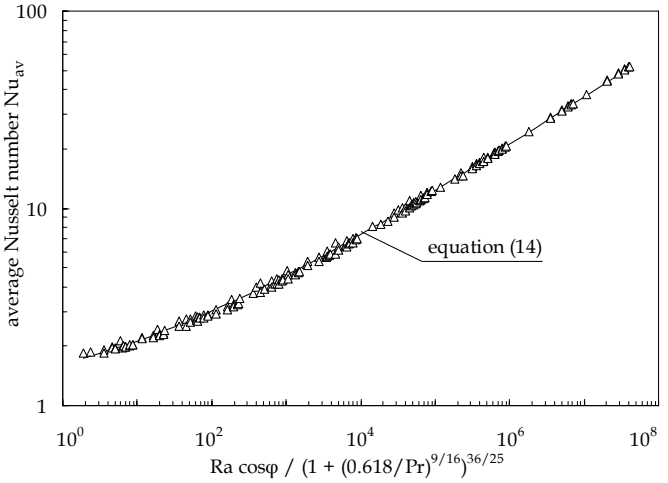

Figure 10 – Correlating equation for the overall heat transfer for tilting angles from –75deg to +60deg

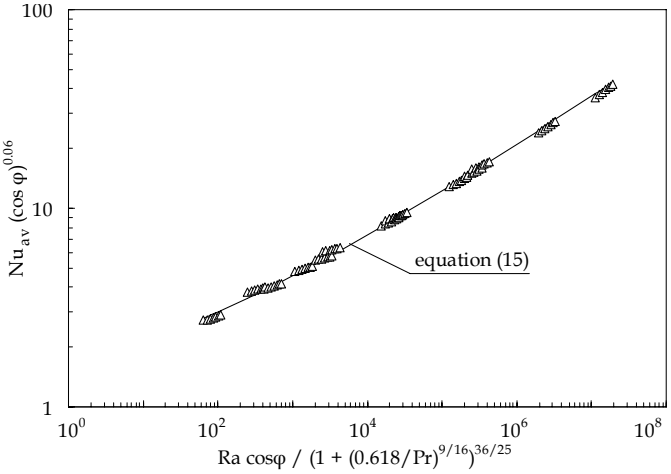

Figure 11 – Correlating equation for the overall heat transfer for tilting angles from +60deg to +75deg

As far as the overall heat transfer performance of the plate is concerned, the following correlating equations are proposed:

$$Nu_{av} = 1 + \frac{0.635}{\left[1 + \left(0.618/\mathrm{Pr}\right)^{9/16}\right]^{9/25}} \left(\mathrm{Ra}\cos\varphi\right)^{0.25} \qquad (14)$$

for $-75\text{deg} \le \varphi < 60\text{deg}$, $5\times10^1 \le \mathrm{Ra} \le 10^8$, and $0.7 \le \mathrm{Pr} \le 70$, with a 2.8% standard deviation of error and a ±7% range of error, as shown in Fig. 10;

$$Nu_{av} = \left\{1 + \frac{0.635}{\left[1 + \left(0.618/\mathrm{Pr}\right)^{9/16}\right]^{9/25}} \left(\mathrm{Ra}\cos\varphi\right)^{0.25}\right\} \frac{1}{\left(\cos\varphi\right)^{0.06}} \qquad (15)$$

for $60\text{deg} \le \varphi \le 75\text{deg}$, $10^3 \le \mathrm{Ra} \le 10^8$, and $0.7 \le \mathrm{Pr} \le 70$, with a 3.3% standard deviation of error, and a ±7% range of error with a 95% level of confidence, as shown in Fig. 11.

CONCLUSIONS

Steady laminar natural convection heat transfer from thin isothermal plates inclined with respect to the gravity vector, for both cases of heated side facing either upwards or downwards, has been studied numerically. Simulations have been executed for different values of the inclination angle of the plate in the range between –75deg and +75deg, the Rayleigh number in the range between 10^1 and 10^8, and the Prandtl number in the range between 0.7 and 70.

The main effect of the inclination angle is the increase in thickness of the boundary layer at the leading or trailing edge of the plate according as the heated side of the plate faces either downwards or upwards. The effects of the Rayleigh and Prandtl numbers are the overall decrease in thickness of the boundary layer, and the shrinkage of the plume, as well as its rotation – outwards with increasing the Rayleigh number, inwards with increasing the Prandtl number.

Finally, dimensionless heat transfer correlating equations of the Churchill-Usagi type have also been developed for both the local and the overall heat transfer performance of the plate.

However, due to the assumption of steady, two-dimensional laminar flow, the present paper should be regarded as a first-stage paper on the subject, which deserves further investigation in order to take into account the influence of three-dimensional effects, e.g., unsteady longitudinal rolls, which in a 2D study are necessarily neglected.

NOMENCLATURE

d	thickness of the plate
g	gravity vector
g	gravitational acceleration
k	thermal conductivity of the fluid
L	length of the plate
Nu	L-based local Nusselt number = $qL/k(t_p - t_\infty)$
Nu_{av}	average Nusselt number = $Q/k(t_p - t_\infty)$
Nu_x	x-based local Nusselt number = $qx/k(t_p - t_\infty)$
p	dimensionless pressure
Pr	Prandtl number = ν/α
Q	heat transfer rate
q	heat flux
Ra	Rayleigh number = $g\beta(t_p - t_\infty)L^3\mathrm{Pr}/\nu^2$
Ra_x	local Rayleigh number = $g\beta(t_p - t_\infty)x^3\mathrm{Pr}/\nu^2$
T	dimensionless temperature
t	temperature
U	dimensionless X-wise velocity component
V	dimensionless Y-wise velocity component
X	dimensionless coordinate parallel to the plate
x	coordinate parallel to the plate
Y	dimensionless coordinate normal to the plate
y	coordinate normal to the plate

Greek symbols

α	thermal diffusivity of the fluid
β	coefficient of volumetric thermal expansion of the fluid

φ tilting angle of the plate with respect to gravity
ν kinematic viscosity of the fluid
ρ density of the fluid

Subscripts
p plate surface
∞ undisturbed fluid

REFERENCES

[1] W. T. Kierkus, An analysis of laminar free convection flow and heat transfer about an inclined isothermal plate, Int. J. Heat Mass Transfer 11 (1968) 241-253.

[2] K. E. Hassan, S. A. Mohamed, Natural convection from isothermal flat surfaces, Int. J. Heat Mass Transfer 13 (1970) 1873-1886.

[3] T. Fujii, H. Imura, Natural convection heat transfer from a plate with arbitrary inclination, Int. J. Heat Mass Transfer 15 (1972) 755-767.

[4] M. Al-Arabi, B. Sakr, Natural convection heat transfer from inclined isothermal plates, Int. J. Heat Mass Transfer 31 (1988) 559-566.

[5] G. C. Vliet, Natural convection local heat transfer on constant-heat-flux inclined surfaces, J. Heat Transfer 91 (1969) 511-516.

[6] G. C. Vliet, D. C. Ross, Turbulent natural convection on upward and downward facing inclined constant heat flux surfaces, J. Heat Transfer 97 (1975) 549-555.

[7] D. E. Fussey, I. P. Warneford, Free convection from a downward facing inclined flat plate, Int. J. Heat Mass Transfer 21 (1978) 119-126.

[8] H. Shaukatullah, B. Gebhart, An experimental investigation of natural convection flow on an inclined surface, Int. J. Heat Mass Transfer 21 (1978) 1481-1490.

[9] J. A. King, D. D. Reible, Laminar natural convection heat transfer from inclined surfaces, Int. J. Heat Mass Transfer 34 (1991) 1901-1904.

[10] M. M. Hasan, R. Eichhorn, Local nonsimilarity solution of free convection flow and heat transfer on an inclined isothermal plate, J. Heat Transfer 101 (1979) 642-647.

[11] T. S. Chen, H. C. Tien, B. F. Armaly, Natural convection on horizontal, inclined, and vertical plates with variable surface temperature or heat flux, Int. J. Heat Mass Transfer 29 (1986) 1465-1478.

[12] J. P. Van Doormaal, G. D. Raithby, Enhancements of the simple method for predicting incompressible fluid flows, Numer. Heat Transfer 11 (1984) 147-163.

[13] B. P. Leonard, A stable and accurate convective modelling procedure based on quadratic upstream interpolation, Comp. Meth. in Appl. Mech. Engng. 19 (1979) 59-78.

[14] S. W. Churchill, H. H. Chu, Correlating equations for laminar and turbulent free convection from a vertical plate, Int. J. Heat Mass Transfer 18 (1975) 1323-1329.

[15] G. D. Raithby, K. G. T. Hollands, Laminar and turbulent free convection from elliptic cylinders, with a vertical plate and horizontal circular cylinder as special case, J. Heat Transfer 98 (1976) 72-80.

[16] S. W. Churchill, R. Usagi, A general expression for the correlation of rates of transfer and other phenomena, A.I.Ch.E. Journal 18 (1972) 1121-1128.